Elliptic flow of baryon-rich matter

Che-Ming Ko
Texas A&M University

- Beam energy scan at RHIC
- Particle and antiparticle elliptic flows
- Hadronic potentials in nuclear medium
- Effects of hadronic potentials on elliptic flow
- Partonic potentials in QGP
- Effects of partonic potentials on elliptic flow
- QCD phase diagram

Based on work with Jun Xu, Lie-Wen Chen & Zi-wei Lin [PRC 85, 041901(R) (2012)]; Taesoo Song, Vincenzo Greco, Salvatore Plumari & Feng Li [arXiv:1211:5511 [nucl-th]]; Xu, Song & Li, [arXiv: 1308.1753 [nucl-th]]

Supported by National Science Foundation and the Welch Foundation

Beam energy scan at RHIC

STAR Collaboration, arXiv: 1007.2613; 1106.5902 [nucl-ex]

- Motivations:

To study QCD phase diagram at finite baryon chemical potential: critical point (CP), onset of de-confinement

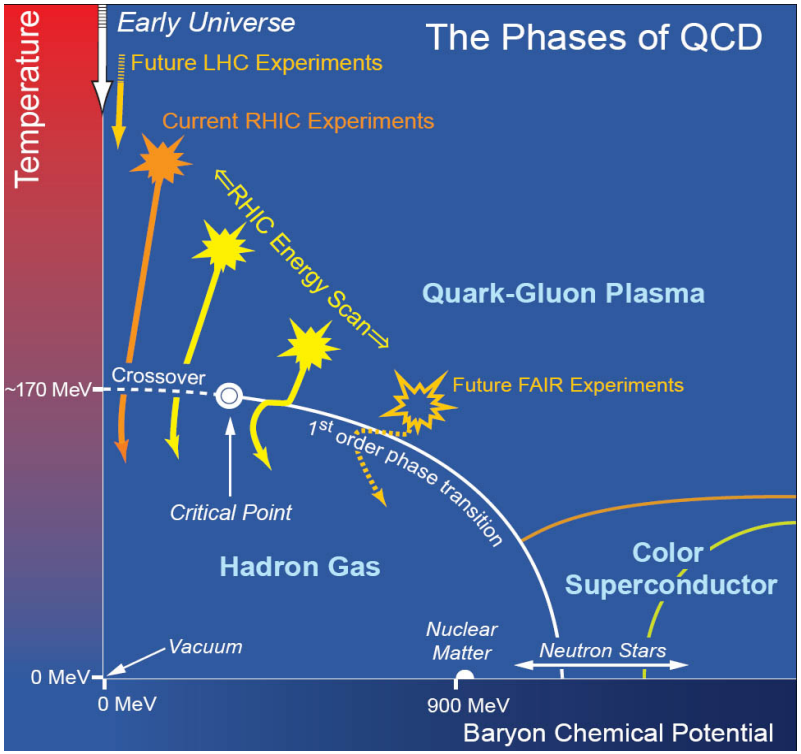

- Experimental observations:

- **Particle ratios**: increasing baryon chemical potential with decreasing beam energy (DBE), reaching ~ 400 MeV at $s^{1/2}_{NN}$ = 7.7 GeV

- **Dynamic charge correlations:** decreasing difference in same and opposite charges correlations with DBE (hadronic dominance?)

- **Freeze-out eccentricity:** increasing with DBE (softening of EOS?)

- **Directed flow:** dv_1/dy changes sign (softening of EOS?) and increasing difference in proton and antiproton dv_1/dy with DBE (hadronic dominance?)

- **Moments of net-proton distributions:** both skewness and kurtosis deviate from HRG for $s^{1/2}_{NN}$ < 39 GeV (presence of CP?)

- **Particle ratio fluctuations:** nonzero $\nu_{dyn}(K/\pi)$ (correlated emission or presence of CP?)

- **Elliptic flow:** breakdown of NCQ scaling and increasing difference between particles and anti-particles with DBE (hadronic dominance? chiral magnetic effect?)

Beam energy dependence of CQN scaled elliptic flow

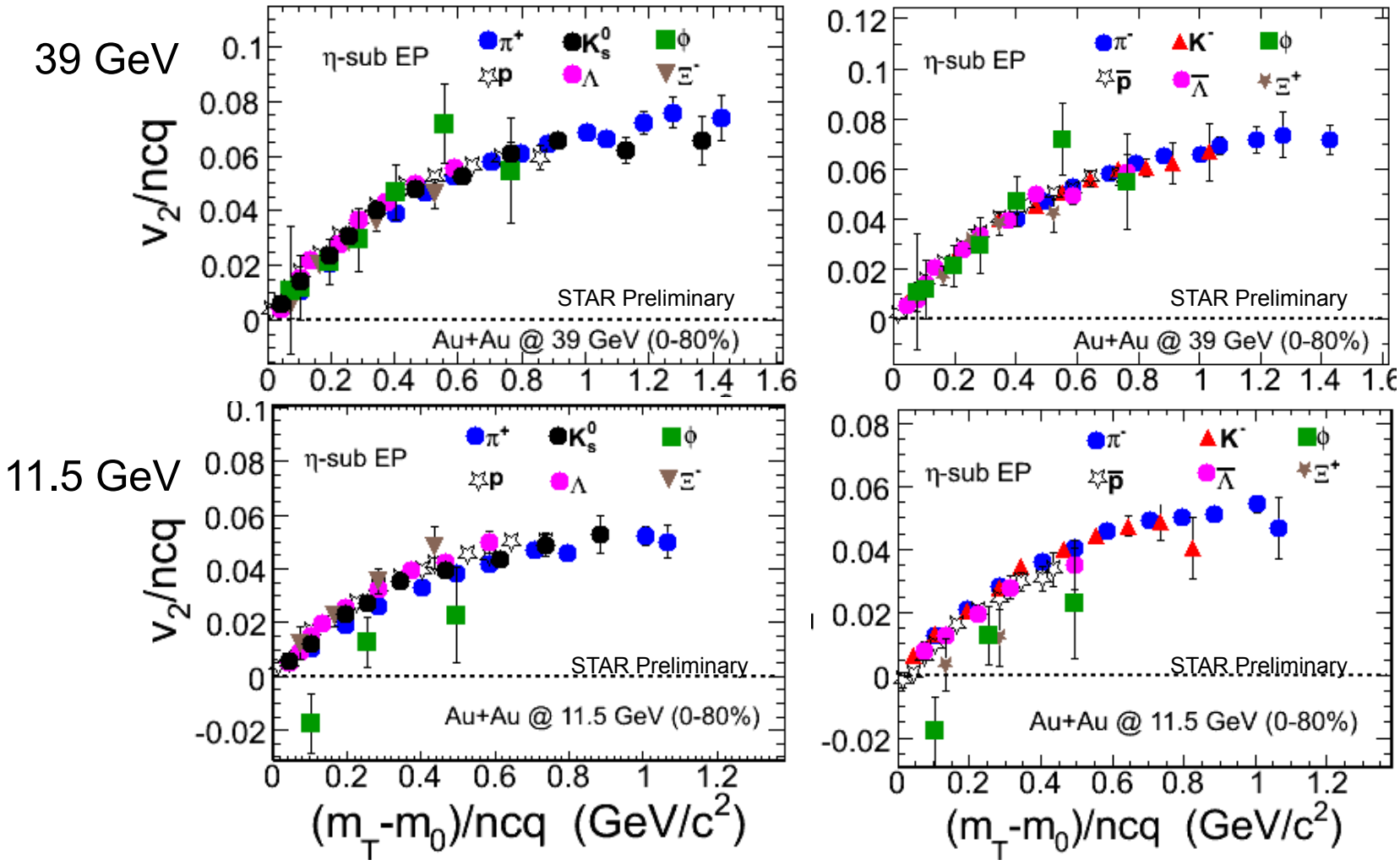

- Phi meson falls off trend at $s^{1/2}_{NN}$ = 11.5 GeV (hadronic dominance?)

Particle and antiparticle elliptic flows

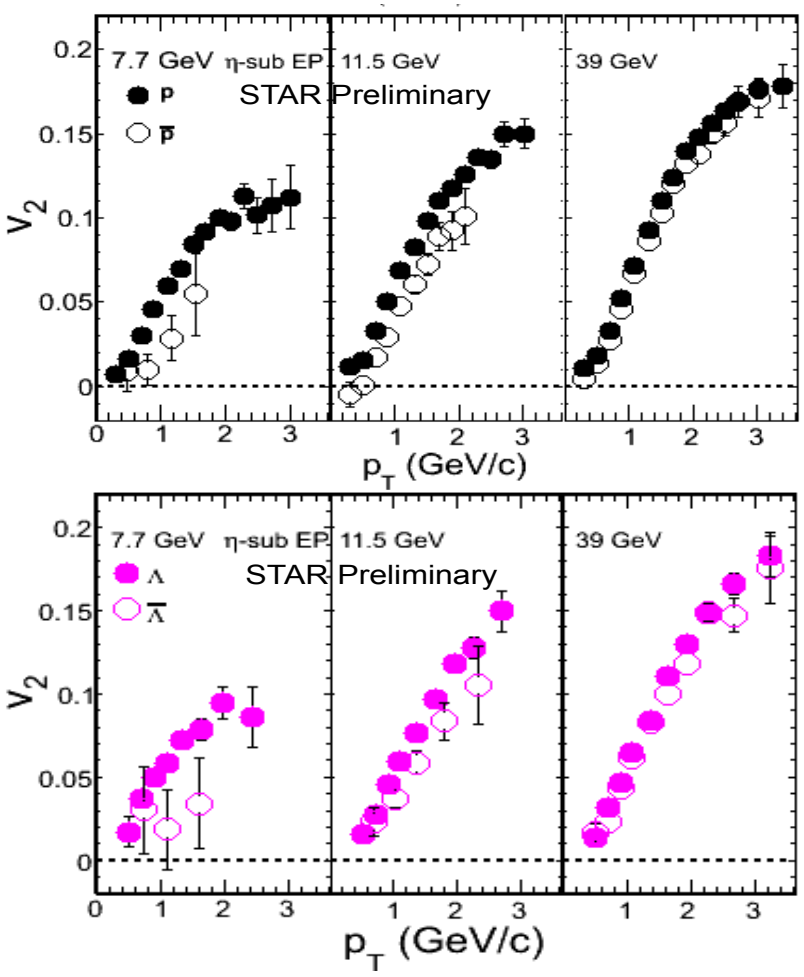

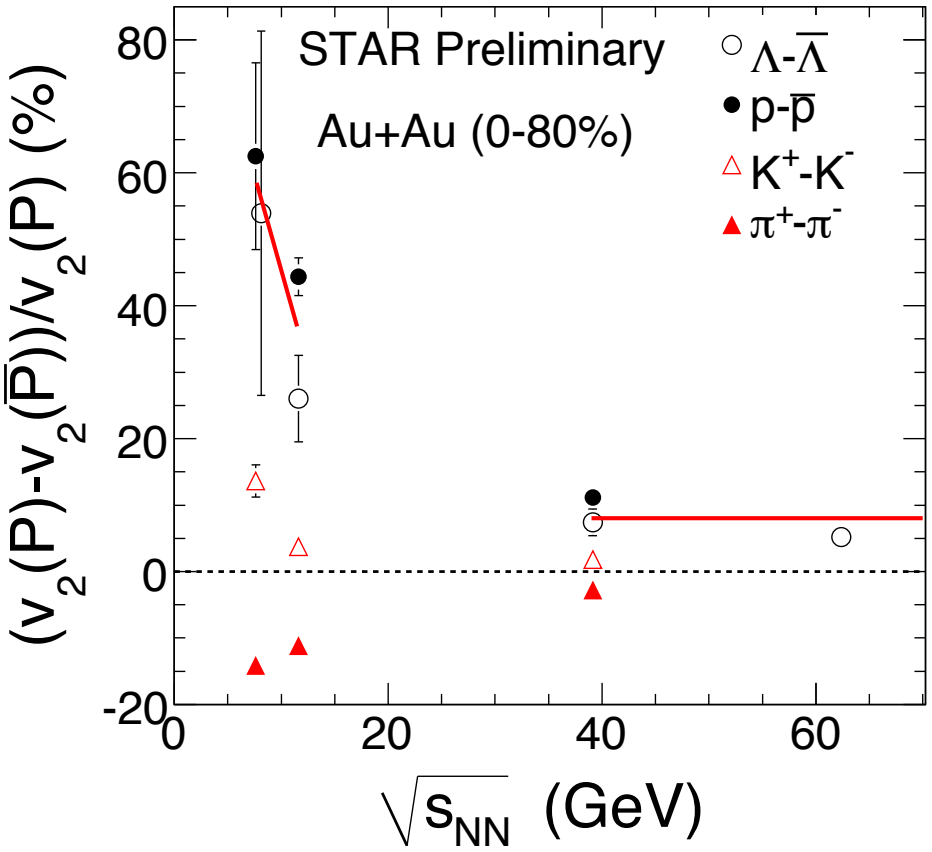

- Particle and antiparticle elliptic flows become significantly different below $s^{1/2}_{NN}$ < 11.5 GeV: v_2(baryon) > v_2(anti-baryon), $v_2(K^+) > v_2(K^-)$, and $v_2(\pi^+) < v_2(\pi^-)$
- P_T-integrated relative v_2 difference between particles and antiparticles: 63%, 44%, and 12% for (p, pbar), 53%, 25%, and 7% for (Λ, Λbar), 13%, 3%, and 1% for (K^+,K^-), -15%, -10%, and -3% for (π^+,π^-) at 7.7, 11.5, and 39 GeV

Possible explanations for different particle and antiparticle elliptic flows

- **Chiral magnetic wave** [Bumier, Kharzeev, Liao & Yee, PRL 107, 052303 (2011)]
  - Stemming from the coupling of the density waves of electric and chiral charge induced by the axial anomaly in the presence of an external magnetic field

    → Electric quadrupole moment in QGP

    → radial flow leads to decreasing positive hadron and increasing negative hadron elliptic flows

    → $v_2(\pi^+) < v_2(\pi^-)$

$$j_V = \frac{N_c e}{2\pi^2}\mu_A B, \quad j_A = \frac{N_c e}{2\pi^2}\mu_V B$$

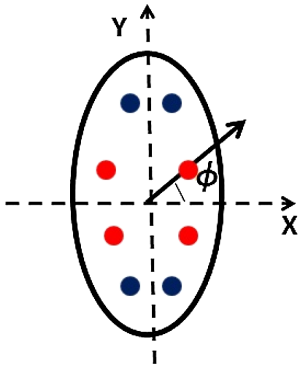

  - Effects on p and $\bar{p}$ as well as K^+ and K^- are masked by different absorption cross sections
- **Transport versus produced particles** [Dunlop, Lisa & Sorensen, PRC 84, 044914 (2011)]: Larger elliptic flow for transport than for produced (anti)particles
- **Different particle and antiparticle transport coefficients** [Greco, Mitrovski & Torrieri, PRC 86, 044905 (2012)] : Large absorption cross sections for antiparticles
- **Baryon charge, strangeness and isospin conservations** [Steinheimer, Koch & Bleicher, PRC 86, 044903 (2012)]: Decreasing pbar/p ratio with radial distance
- **Different particle and antiparticle potentials** [Xu, Chen, Lin & Ko, PRC 85, 041901(R) (2012)]: Repulsive potential for particles and attractive potential for antiparticles
- **Different quark and antiquark potentials** [Song, Plumari, Greco, Ko &Li, arXiv:1211.5511 [nucl-th]]: Repulsive vector potential for quarks and attractive one for antiquarks

Hadronic potentials in nuclear medium (I)

Ko & Li, JPG 22, 1673 (1996); Ko, Koch & Li, ARNPS 47, 505 (1997)

- **Nucleons and antinucleons:** Relativistic mean-field model → attractive scalar potential Σ_s and repulsive vector potential Σ_v ("+" for nucleons and "-" for antinucleons due to G-parity)

$$U_{N,\bar{N}}(\rho_s,\rho_B) = \Sigma_s(\rho_s,\rho_B) \pm \Sigma_v^0(\rho_s,\rho_B) = \frac{g_\sigma^2}{m_\sigma^2}\rho_s \pm \frac{g_\omega^2}{m_\omega^2}\rho_B$$

$$U_N = -60 \text{ MeV}, U_{\bar{N}} = -260 \text{ MeV at } \rho_0 = 0.16 \text{ fm}^{-3}$$

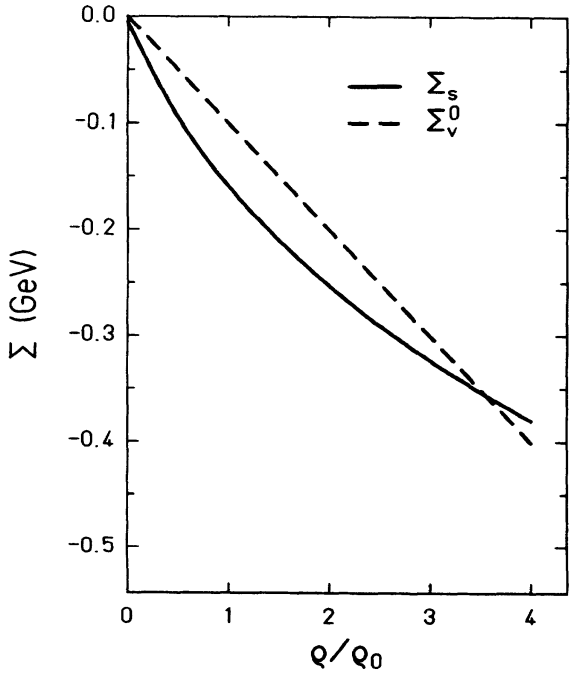

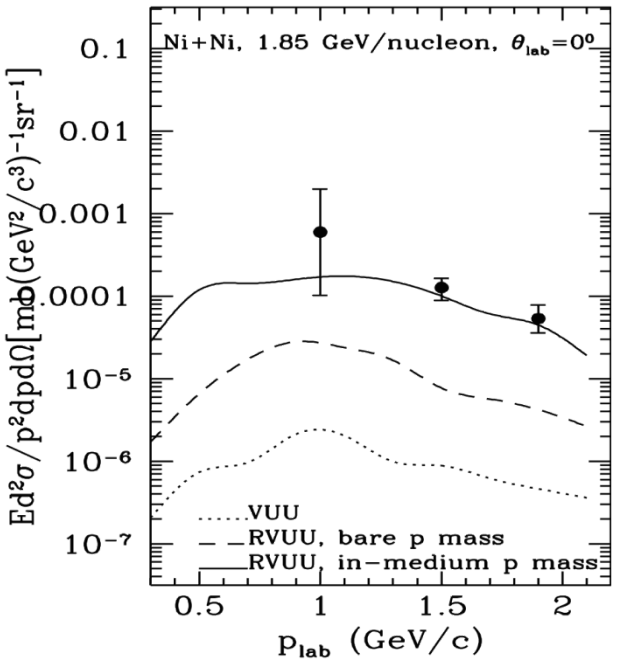

- Deep antiproton attractive potential reduces its production threshold and thus enhances its yield in subthreshold heavy ion collisions

Hadronic potentials in nuclear medium (II)

Ko & Li, JPG 22, 1673 (1996); Ko, Koch & Li, ARNPS 47, 505 (1997)

- **Kaons and antikaons:** Chiral effective Lagrangian → repulsive potential for kaons and attractive potential for antikaons

$$U_{K,\bar{K}} = \omega_{K,\bar{K}} - \omega_0, \quad \omega_0 = \sqrt{m_K^2 + p^2}$$

$$\omega_{K,\bar{K}} = \sqrt{m_K^2 + p^2 - a_{K,\bar{K}}\rho_s + \left(b_K \rho_B\right)^2} \pm b_K \rho_B$$

$$a_K = 0.22\ \text{GeV}^2\text{fm}^3, \quad a_{\bar{K}} = 0.45\ \text{GeV}^2\text{fm}^3$$

$$b_K = 0.33\ \text{GeV}^2\text{fm}^3$$

$$\Rightarrow \quad U_K = 20\ \text{MeV}, U_{\bar{K}} = -120\ \text{MeV at } \rho_0 = 0.16\ \text{fm}^{-3}$$

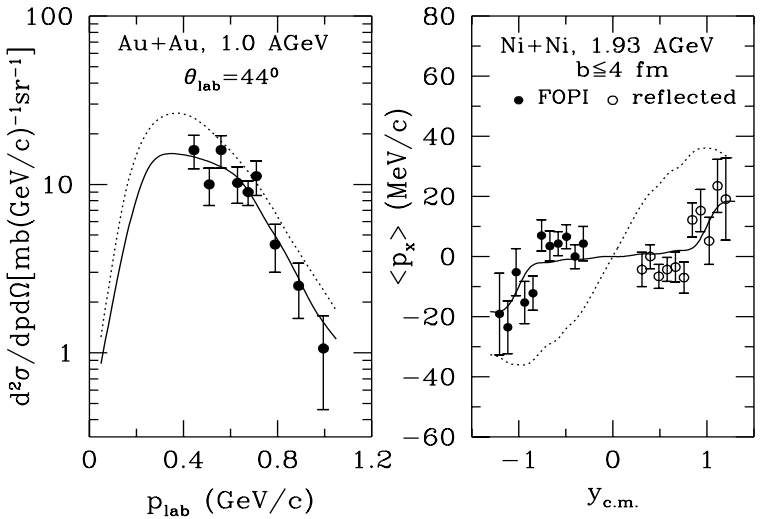

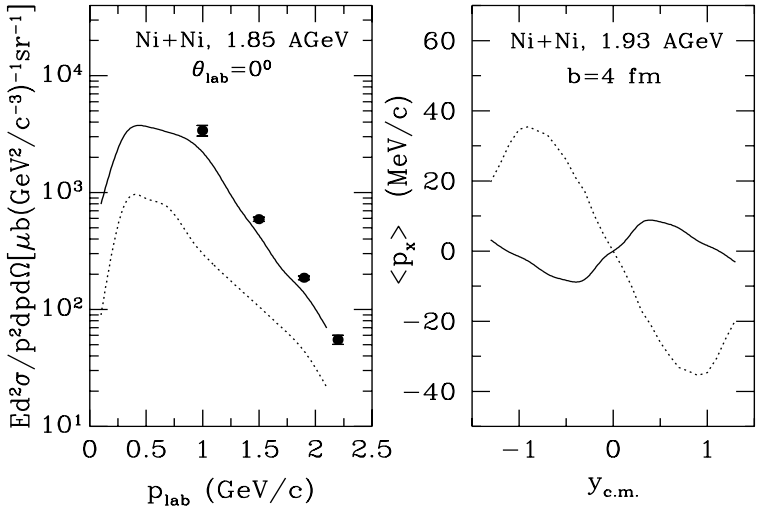

- Experimental data on spectrum and directed flow are consistent with repulsive kaon and attractive antikaon potentials

Hadronic potentials in nuclear medium (III)

Kaiser & Weise,
PLB 512, 283 (2001)

- **Pions**: $U_\pi = \Pi/(2m_\pi)$ in terms of pion selfenergies

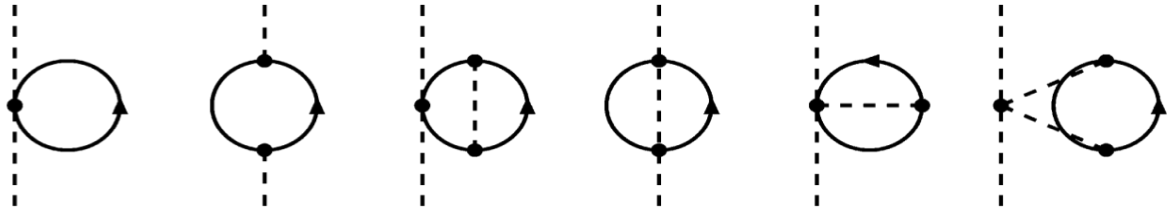

$$\Pi^-(\rho_n,\rho_p) = \rho_n[T^-_{\pi N} - T^+_{\pi N}] - \rho_p[T^-_{\pi N} + T^+_{\pi N}] + \Pi^-_{\rm rel}(\rho_n,\rho_p) + \Pi^-_{\rm cor}(\rho_n,\rho_p)$$

$$\Pi^+(\rho_p,\rho_n) = \Pi^-(\rho_n,\rho_p)$$

$$\Pi^0(\rho_n,\rho_p) = -(\rho_p+\rho_n)T^+_{\pi N} + \Pi^0_{\rm cor}(\rho_n,\rho_p)$$

Isospin even and odd πN-scattering matrices extracted from energy shift and width of 1s level in pionic hydrogen atom

$$T^+_{\pi N} \approx 1.847\,\text{fm} \quad \text{and} \quad T^-_{\pi N} \approx -0.045\,\text{fm}$$

At normal nuclear density ρ=0.165 fm^{-3} and isospin asymmetry δ=0.2 such as in Pb,

$$U_{\pi^-} = 14\ \text{MeV},\ U_{\pi^+} = -1\ \text{MeV},\ U_{\pi^0} = 6\ \text{MeV}$$

Hadron density evolutions in AMPT

Adjust parton scattering cross section and ending time of partonic stage to approximately reproduce measured elliptic flows and extracted hadronic energy density (~ 0.35 GeV/fm^3): isotropic cross sections of 3, 6 and 10 mb, and parton ending time of 3.5, 2.6, 2.9 fm/c for $s^{1/2}_{NN}$= 7.7, 11.5, and 39 GeV, respectively

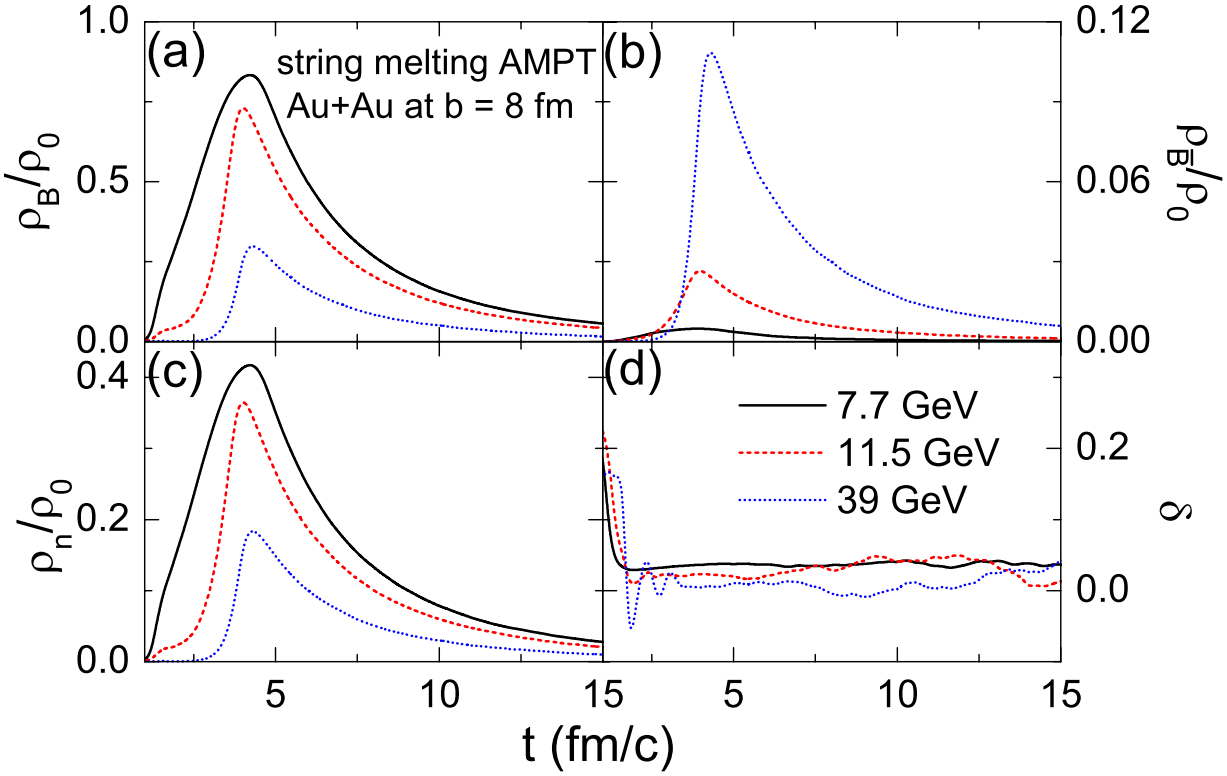

- Increasing baryon and decreasing antibaryon densities with decreasing energy
- Increasing neutron density with decreasing energy, but isospin asymmetry δ=0.02 is small due to production of Λ hyperon and pions

Particle and antiparticle differential elliptic flows

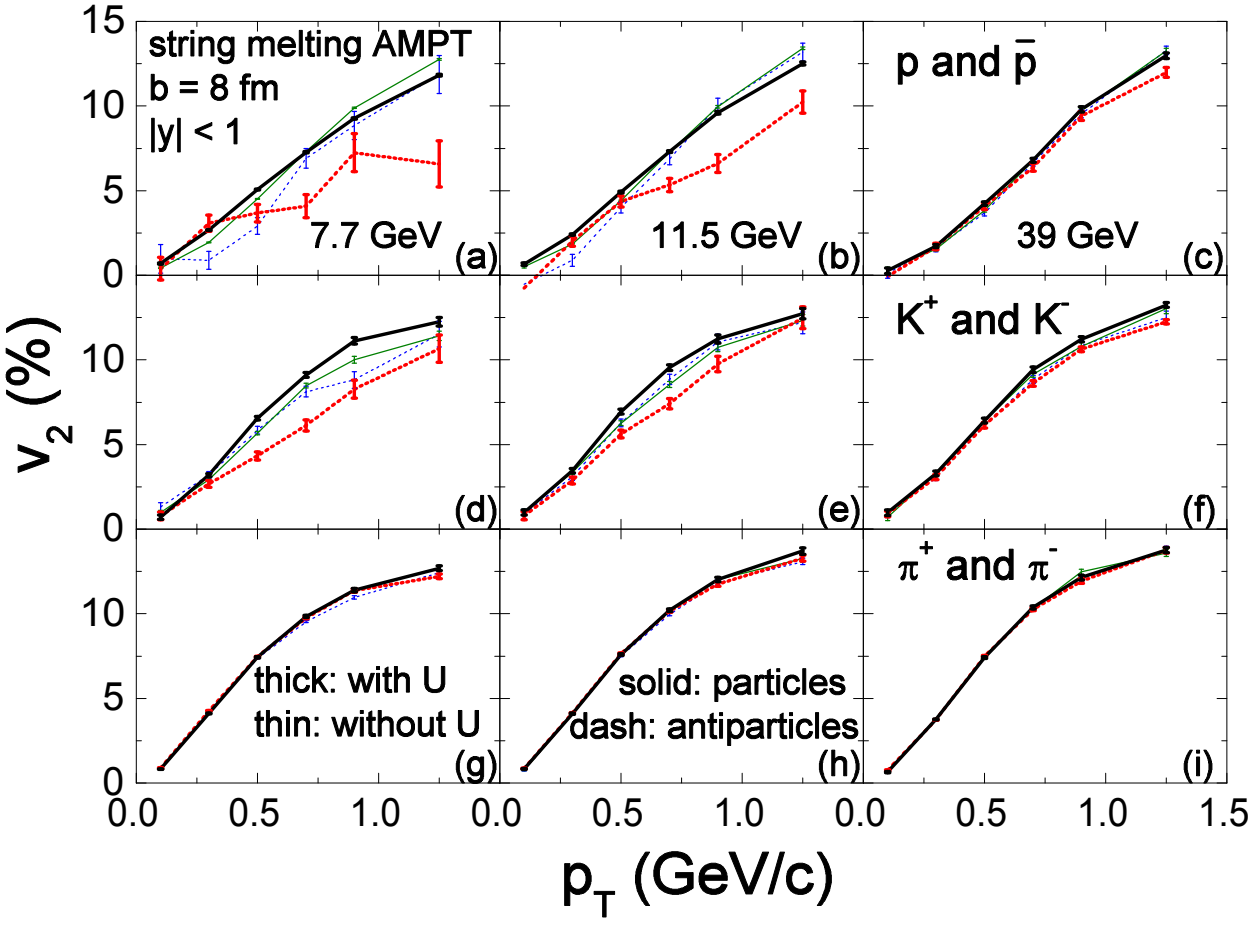

- Similar particle and antiparticle elliptic flows without hadronic potentials
- Hadronic potentials increase slightly p and pbar v_2 at p_T<0.5 GeV but reduce slightly (strongly) p (pbar) v_2 at high p_T
- Hadronic potentials increase slightly v_2 of K^+ and reduce v_2 of K^-
- Effects of hadronic potentials on π^+ and π^- v_2 are small

P_T-integrated particle and antiparticle elliptic flow difference

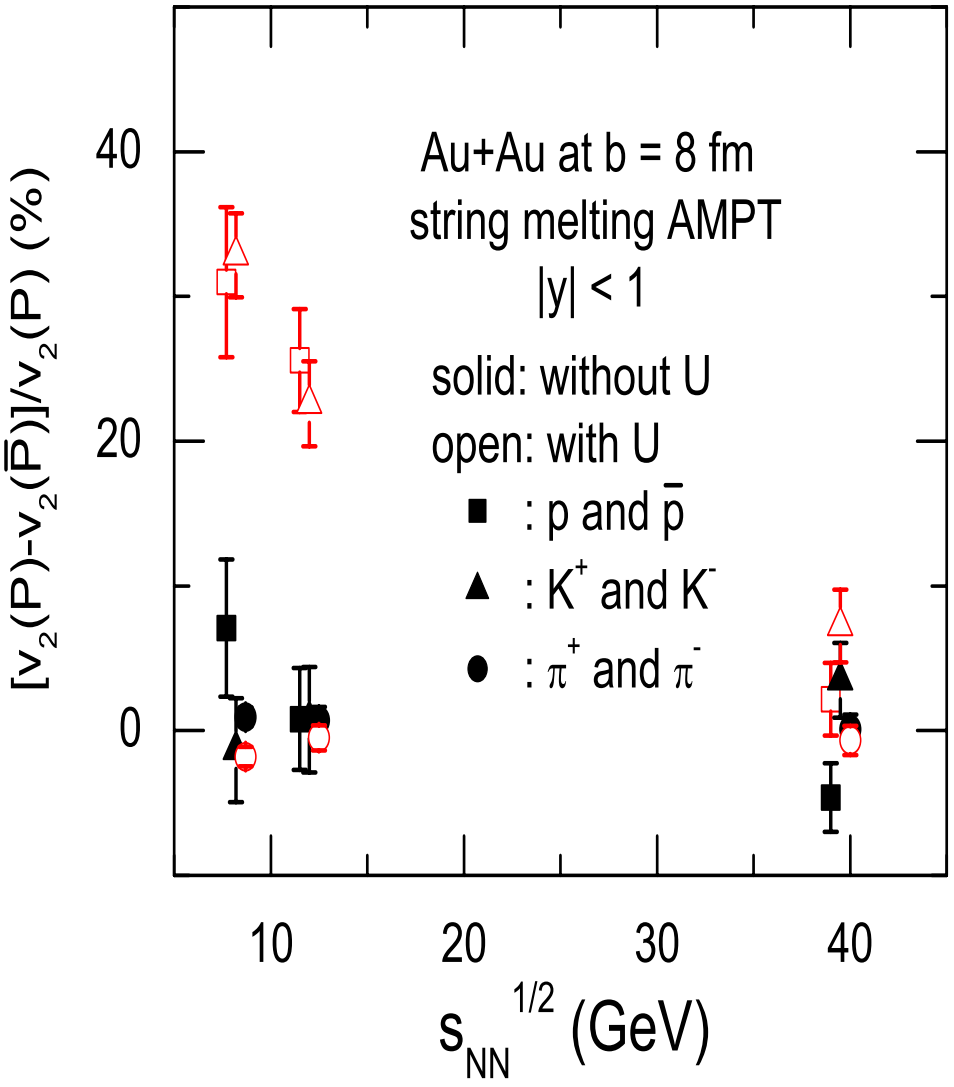

→ Hadronic potentials underestimate p-pbar and overestimate K^+-K^- v_2 difference

- Difference very small without hadronic potentials → different particle and antiparticle scattering and absorption cross sections have small effects
- Hadronic potentials lead to relative v_2 difference between p and pbar and between K^+ and K^- of 30% at 7.7 GeV, 20% at 11.5 GeV, and negligibly small value at 39 GeV, only very small negative value between π^+ and π^-
- Compared to experimental values of 63%, 44%, and 12% for (p,pbar), 13%, 3%, and 1% for (K^+,K^-), -15%, -10%, and -3% for (π^+,π^-) at 7.7, 11.5, and 39 GeV, ours are smaller for (p,pbar) and (π^+,π^-) and larger for (K^+,K^-)

Quark and antiquark potentials in QGP (I)

- NJL model [Bratovic, Hatsuda & Weise, PLB 719, 131 (2013)]

$$\mathcal{L} = \bar{\psi}(i\not{\partial} - M)\psi + \frac{G}{2}\sum_{a=0}^{8}\left[(\bar{\psi}\lambda^a\psi)^2 + (\bar{\psi}i\gamma_5\lambda^a\psi)^2\right]$$

Scalar-pseudoscalar

$$+\sum_{a=0}^{8}\left[\frac{G_V}{2}(\bar{\psi}\gamma_\mu\lambda^a\psi)^2 + \frac{G_A}{2}(\bar{\psi}\gamma_\mu\gamma_5\lambda^a\psi)^2\right]$$

Vector-axial vector

$$-K\left[\det{}_f\left(\bar{\psi}(1+\gamma_5)\psi\right) + \det{}_f\left(\bar{\psi}(1-\gamma_5)\psi\right)\right],$$

Kobayashi-Maskawa-t'Hooft (KMT)

where $\det_f(\bar{\psi}\Gamma\psi) = \sum_{i,j,k}\varepsilon_{ijk}(\bar{u}\Gamma q_i)(\bar{d}\Gamma q_j)(\bar{s}\Gamma q_k).$

- Mean-field approximation

$$\mathcal{L} = \bar{\psi}\left(i\partial^\mu - \frac{2}{3}G_V\langle\bar{\psi}\gamma^\mu\psi\rangle\right)\gamma_\mu\psi - \bar{\psi}M^*\psi + ...$$

where M* = diag(M_u, M_d, M_s) with

$$M_u = m_u - 2G\langle\bar{u}u\rangle + 2K\langle\bar{d}d\rangle\langle\bar{s}s\rangle$$
$$M_d = m_d - 2G\langle\bar{d}d\rangle + 2K\langle\bar{s}s\rangle\langle\bar{u}u\rangle$$
$$M_s = m_s - 2G\langle\bar{s}s\rangle + 2K\langle\bar{u}u\rangle\langle\bar{d}d\rangle$$

$$\langle\bar{q}_i q_i\rangle = -2M_i N_c\int\frac{d^3\mathbf{k}}{(2\pi)^3 E_i}\,[1 - f_i(k) - \bar{f}_i(k)]$$

$$\langle\bar{\psi}\gamma^\mu\psi\rangle = 2N_c\sum_{i=u,d,s}\int\frac{d^3\mathbf{k}}{(2\pi)^3 E_i}\,k^\mu[f_i(k) - \bar{f}_i(k)],$$

Quark and antiquark potentials in QGP (II)

$$U_{q,\bar{q}} = \sqrt{M_q^2 + (\vec{p} \mp g_v \vec{\rho})^2} \pm g_v \rho_0 - \sqrt{m_q^2 + \vec{p}2}$$

Net baryon current: $\vec{\rho} = \langle \bar{\psi} \vec{\gamma} \psi \rangle$

Net baryon density: $\rho_0 = \langle \bar{\psi} \gamma^0 \psi \rangle$

$$g_v = \frac{2}{3} G_V$$

- Quark mass is modified by the quark condensate
  - attractive scalar potential on both quark and antiquark
- Vector potential is repulsive for quark and attractive for antiquark
  - enhances relative v_2 difference between quarks and antiquarsk
  - enhances relative v_2 difference between p and pbar, Λ and Λbar, K^+ and K^-

→ Would bring results with only hadronic potentials closer to experimental data

Effects of attractive scalar potential in quark matter

Plumari, Baran, Di Tori, Ferini, and Greco, PLB 689, 18 (2010)

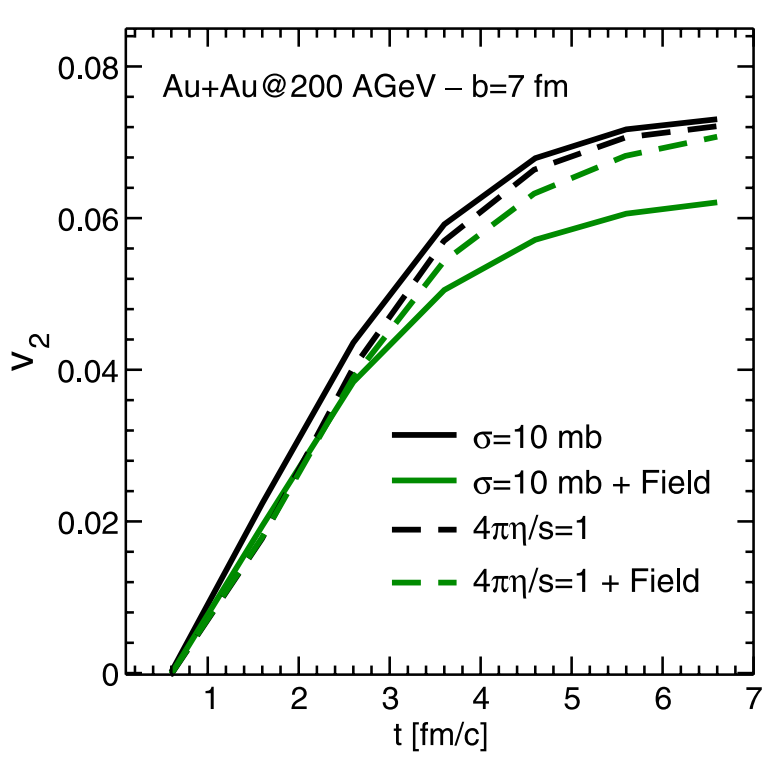

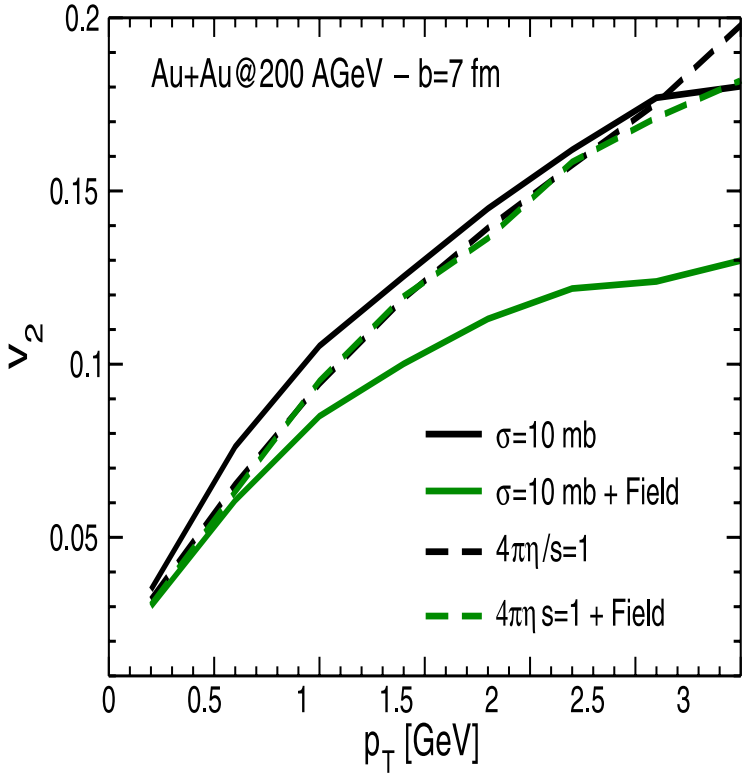

- Attractive scalar potential reduces v_2 of both quark and antiquark
- Effects are reduced when parton scattering cross section is large

Effects of vector potential in quark matter

Using $m_u = m_d = 3.6$ MeV, $m_s = 87$ MeV, $G\Lambda^2 = 3.6$, $K\Lambda^5 = 8.9$, $\Lambda = 750$ MeV

Initial parton distributions from AMPT

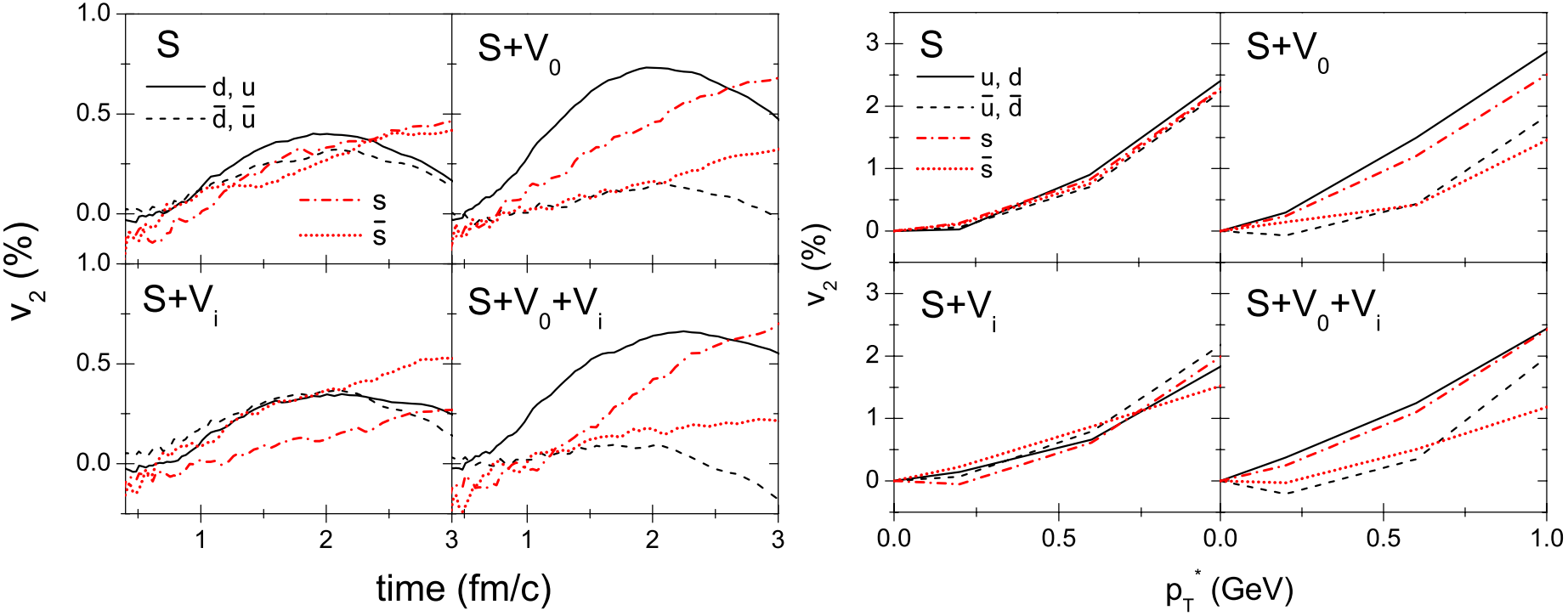

- Time (electric) component of vector potential increases quark but decreases antiquark elliptic flows
- Space (magnetic) component of vector potential has a similar effect at low p_T but an opposite effect at high p_T
- Net effect of vector potential: larger quark than antiquark elliptic flows

Partonic mean-field effects on hadron and antihadon v_2

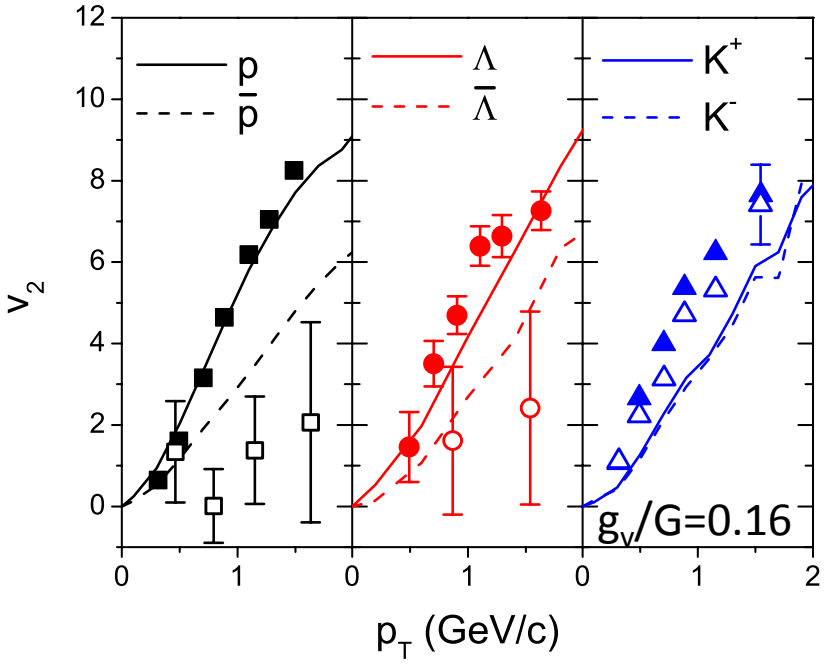

- Using recombination (coalescence) model to produce hadrons (proton, lambda, kaon) and their anitparticles from quarks and antiquarks at hadronization
- Smaller antiquark than quark v_2 leads to smaller v_2 for antiproton than proton, antilambda than lambda, and K^- than K^+

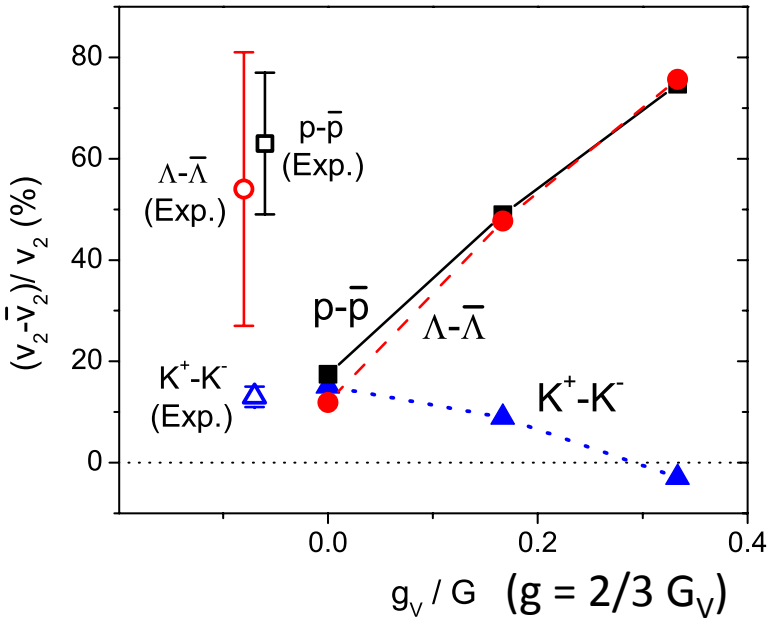

- Relative v_2 differences between proton and antiproton, lambda and antilambda, increase almost linearly with the strength of quark vector interaction
- Relative v2 difference between K^+ and K^- decreases with the strength of quark vector interaction

Effects of hadronic evolution (mean fields + scattering)

Before hadronic evolution

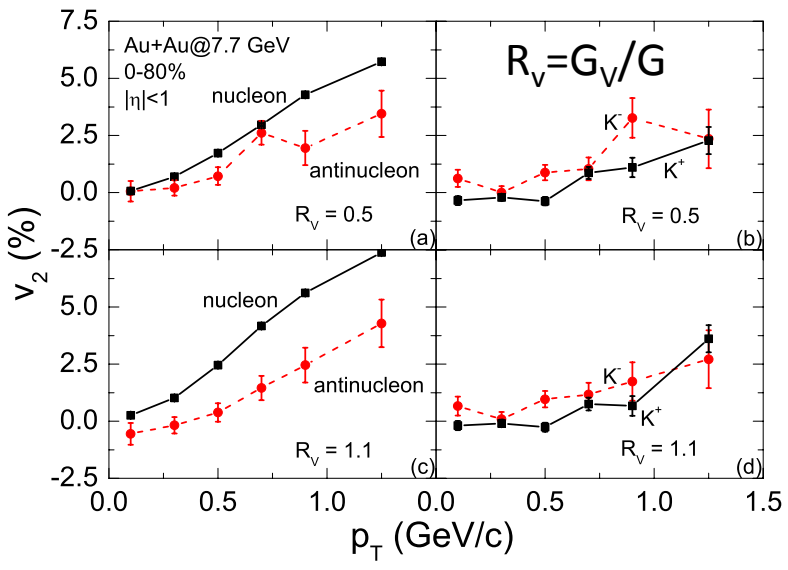

After hadronic evolution

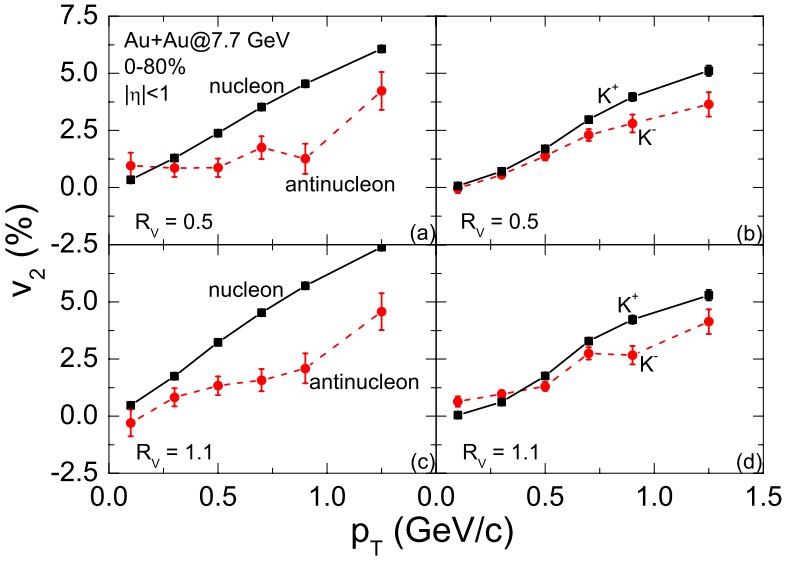

- Before hadronic evolution
  - nucleons have larger v_2 than antinucleons
  - K^- have larger v_2 than K^+
- After hadronic evolution
  - v_2 increases for all hadrons
  - v_2 of nucleons remains larger than that of antinucleons
  - v_2 of K^+ becomes larger than that of K^-

Charged hadron elliptic flow

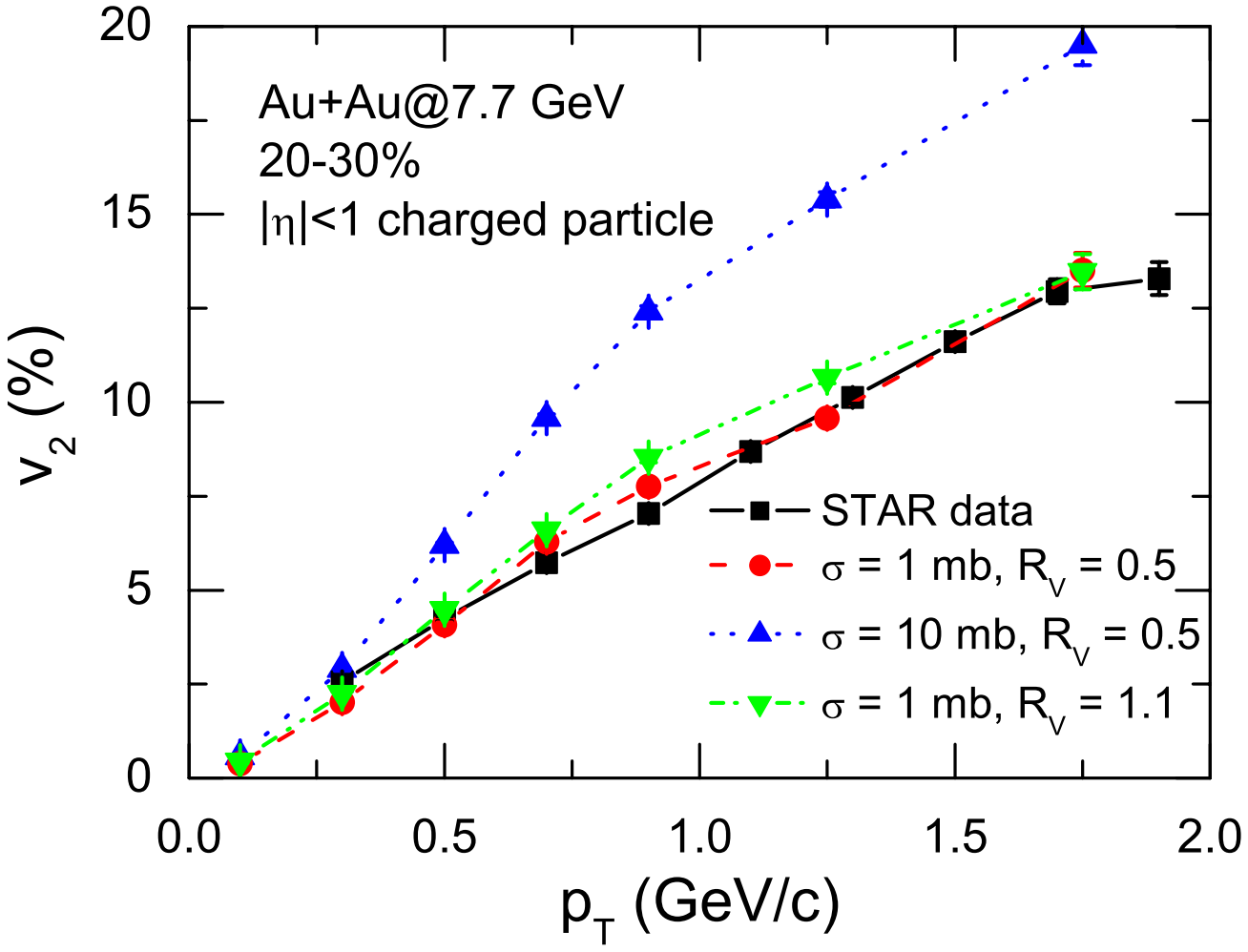

- Sensitive to parton cross section → 1 mb to reproduce data
- Insensitive to partonic vector mean fields

Relative v_2 difference including both partonic and hadronic potentials

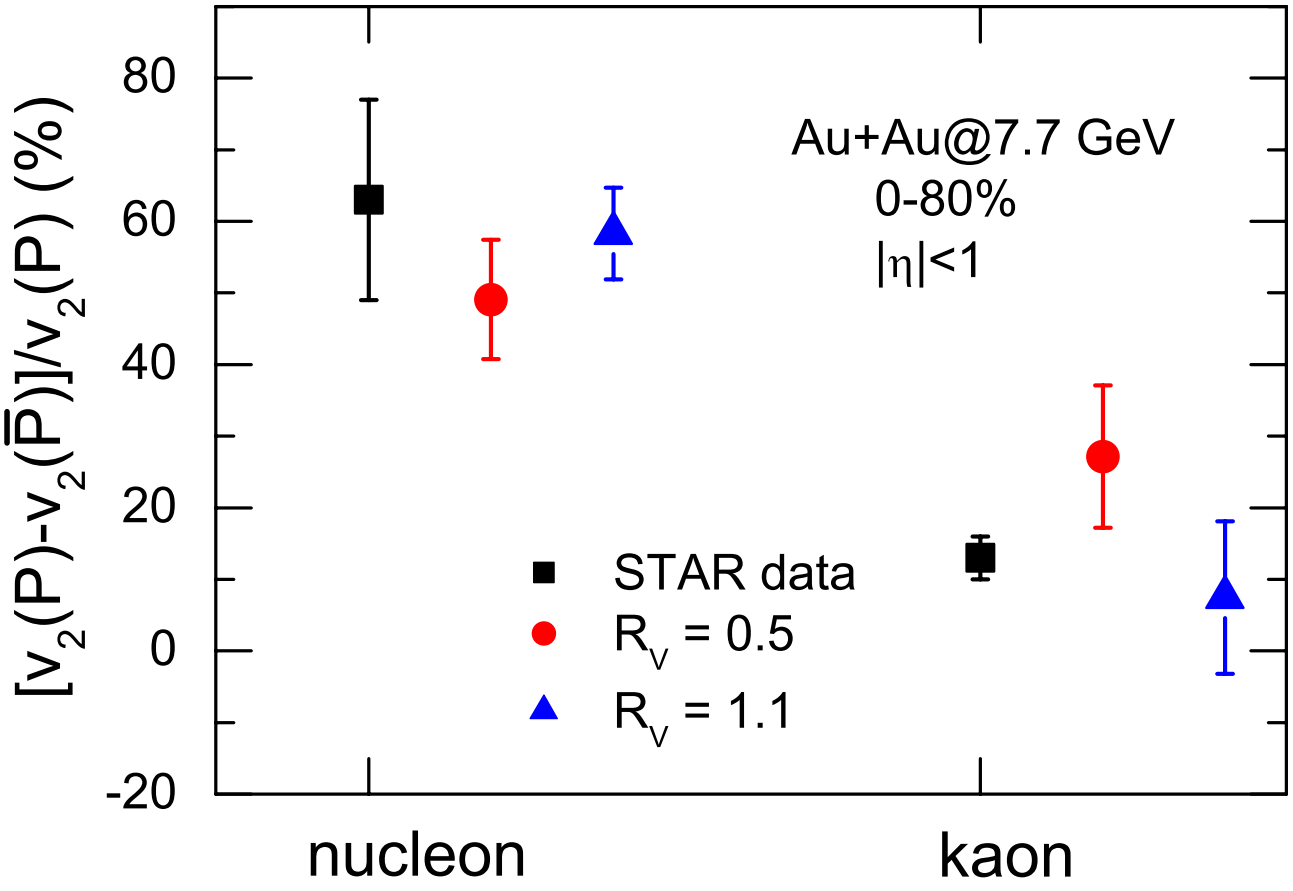

- Finite partonic vector mean field with G_v/G=0.5 -1.1 is needed to describe STAR data

Effects of vector interaction on QCD phase diagram

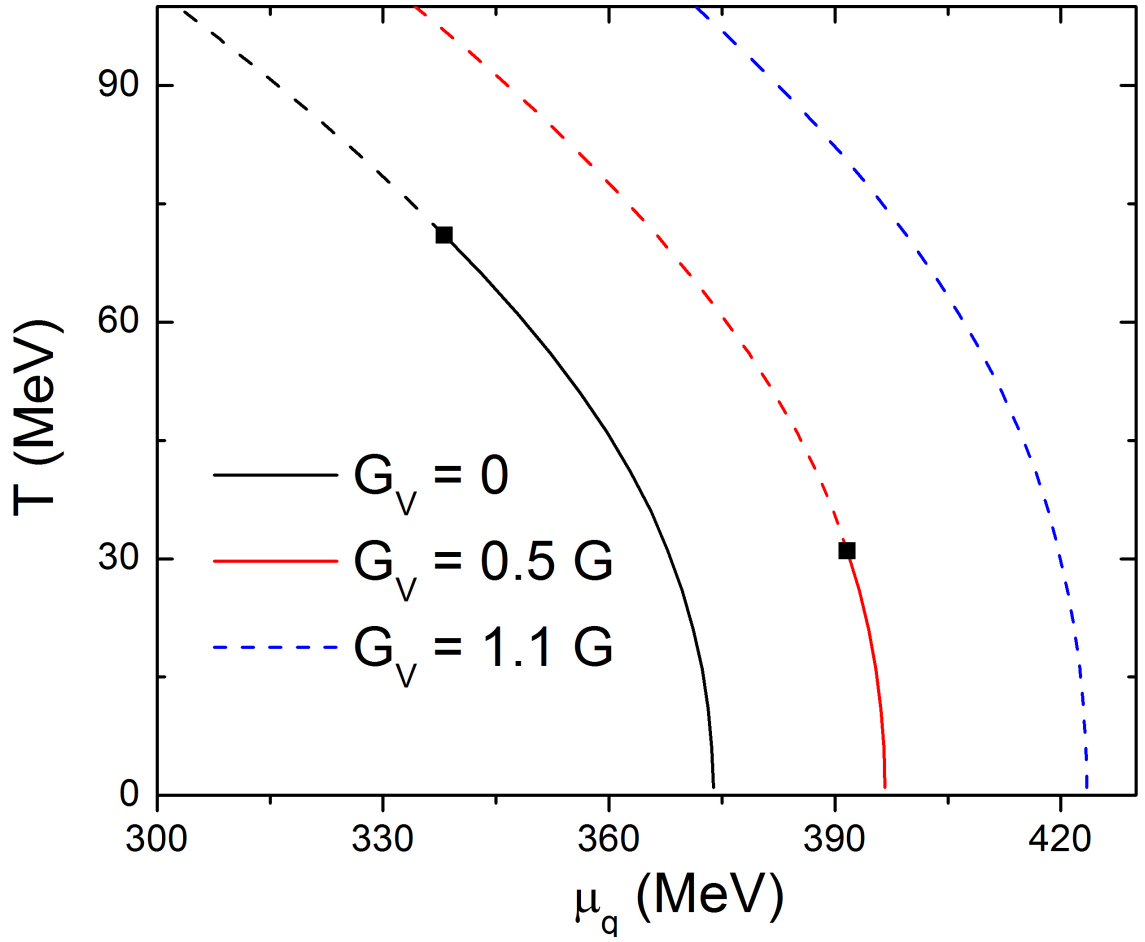

- Location of critical point depends strongly on G_V; moving to lower temperature and larger baryon chemical potential as G_V increases
- Critical point disappears for $G_V > 0.6\ G$

Summary

- Different particle and antiparticle v_2 is observed in BES at RHIC where produced matter has a large finite baryon chemical potential (~ 400 MeV)
- Taking into account different potentials for hadrons and antihadrons can partially account for the experimental observation
- Quarks and antiquarks are affected by scalar and vector potentials in QGP
  - reduced v_2 due to attractive scalar potential
  - vector potential becomes nonzero at finite baryon chemical potential; repulsive for quarks and attractive for anitquarks
  - larger quark than antiquark v_2 in baryon-rich QGP
  - larger v_2 for proton than antiproton, lambda than antilambda, and K^+ than K^- (small G_V) or K^- than K^+ (large G_V) after hadronization
- Including both partonic and hadronic potentials → G_V = 0.5 -1.1 G

  → absence of critical point in QCD phase diagram?
- Information on quark and antiquark potentials at finite baryon chemical potential is useful for understanding the phase structure of QCD